Available online at www.sciencedirect.com
ScienceDirect
Journal of Organometallic Chemistry 693 (2008) 1957–1967
Journal of Organometallic Chemistry
www.elsevier.com/locate/jorganchem

An investigation of the formation of 1,3,5-heterosubstituted benzene rings by cyclo-condensation of acetyl-substituted organometallic complexes

Francis O. Ogini [a], Yanick Ortin [b], Amir H. Mahmoudkhani [a], Anthony F. Cozzolino [a], Michael J. McGlinchey [b,*], Ignacio Vargas-Baca [a,*]

[a] Department of Chemistry, McMaster University, 1280 Main Street West, Hamilton, Ontario, Canada L8S 4M1
[b] School of Chemistry and Chemical Biology, University College Dublin, Belfield, Dublin 4, Ireland

Received 13 February 2008; accepted 13 February 2008
Available online 20 February 2008

Abstract

The cyclocondensation of acetylferrocene and acetylcymantrene catalyzed by $SiCl_4$ in ethanol yields a mixture of 1,3,5-trisubstituted benzenes and the intermediate 3,1-disubstituted (*E*)-2-buten-1-ones, including all the homo- and heterometallic species, which were separated and quantified by HPLC. The relative yields of these species are determined by the different ability of the organometallic groups to stabilize the cationic intermediates that participate in the reaction mechanism, which is measurable as the basicity of the starting materials. The X-ray crystal structures of 1-cymantrenyl-3,5-diferrocenylbenzene and (*E*)-3-cymantrenyl-1-ferrocenyl-2-buten-1-one are described within this report.

Keywords: Organometallic ketones; Cyclocondensation; Hetero-organometallics; pK_a measurements; HPLC

1. Introduction

Molecules consisting of conjugated backbones that bridge organometallic groups offer a wide variety of electrochemical, spectroscopic (absorption and luminescence), electronic and optical properties that are of fundamental interest and hold the potential for practical applications [1]. While most of the work in this area has been concerned with homometallic systems, there are instances in which it is desirable to incorporate different metal centers in the same molecule [2]. For example, all-organometallic second-order nonlinear optical chromophores can be built using organometallic functional groups for both the electron donor and the electron acceptor extremes of molecules with a traditional dipolar D–π–A architecture [3].

Second-order nonlinear optical activity is not confined to molecules with permanent dipole moments. Noncentrosymmetric non-polar molecules do exhibit significant octupolar nonlinear optical responses [4], examples of these possess tetrahedral structures or a ternary symmetry (e.g., C_{3v}, D_{3h}). In this respect, there has been great interest in aromatic molecules such as 1,3,5-triazines and 1,3,5-substituted benzenes (**1**; see Chart 1 for all structures), some of them with organometallic substituent groups [5].

Of the several methods available to prepare 1,3,5-substituted benzene rings, few combine the simplicity and versatility of the catalytic cyclo-trimerization of alkynes [6] and the cyclo-condensation of ketones and aldehydes [7]. However, these methods do have some complications. While competing polymerization is not usually observed (except with Schrock-type carbene catalysts [8]), cyclotrimerization of alkynes usually gives the 1,2,4- and 1,3,

* Corresponding authors. Tel.: +1 905 525 9140; fax: +1 905 522 2509 (I. Vargas-Baca), tel.: +353 1 716 2880; fax: +353 1 716 1178 (M.J. McGlinchey).
E-mail addresses: michael.mcglinchey@ucd.ie (M.J. McGlinchey), vargas@chemistry.mcmaster.ca (I. Vargas-Baca).

0022-328X/$ - see front matter © 2008 Elsevier B.V. All rights reserved.
doi:10.1016/j.jorganchem.2008.02.013

5-substitution isomers when catalyzed by disilanes and transition metal compounds [9]. On the other hand, the cyclo-condensation of carbonylic compounds often yields a complex mixture which includes intermediates formed along a process consisting of a series of nucleophilic addition and α-substitution steps (Scheme 1) which are not always efficient; typically, the yield of 1,3,5-triphenylbenzene from acetophenone does not exceed 20–50% [10]. Although acid and base catalysts have both been implemented to induce this transformation, acid-type catalysts are more commonly used [11]. The first stage in the sequence is the aldol condensation enabled by the protonation and the enolization equilibria of a methyl ketone, **2**. Formation of the α,β-unsaturated ketone **3**, is facilitated by the enhanced electrophilicity of the protonated ketone, **4**. Under acidic conditions, **3** can enolize and undergo a second aldol condensation with another molecule of **2**; this is followed by dehydration. The resulting chain is made up of three ketone or aldehyde molecules. Such trimeric species can then cyclize by performing an internal aldol condensation and dehydration, with the strong driving force from the aromaticity of the benzene ring. Naturally, removal of water from the reaction mixture drives the overall process forward, even though the initial aldol condensation is unfavorable for ketones. Therefore, the best catalysts for this process are those Brønsted or Lewis acids which also act as dehydrating agents, for example H_2SO_4, $ZnCl_2$, polyphosphoric acid, BF_3, $BeCl_2$, $AlCl_3$, $AlBr_3$, and anhydrous HCl.

This approach can be extended to the preparation of unsymmetrically substituted benzenes [12]. For example, hetero-triannulated benzenes such as 2,3,4,5,6,7,8,9,10,11-decahydro-1*H*-cyclopenta[*l*]phenanthrene and 1,2,3,4,5,6,7,8,9,10-decahydrobenzen[*e*]-*as*-indacene [13] can be prepared from preformed enones in the presence of cyclopentanone or cyclohexanone, and $CuCl_2$. However, the products of unsymmetrical substitution are not necessarily selected by the relative proportions of starting materials. The equilibria of protonation and tautomerization can impose thermodynamic and kinetic barriers that could override the mere influence of stoichiometry. This is specially significant when the ketones include pendant organometallic groups, which are better at stabilizing the carbocationic intermediates of cyclo-condensation than purely organic substituents [14], but it is uncertain how exactly this ability would influence the yields of the reaction.

Many of the reports on the cyclocondensation of organometallic ketones have focused on ferrocenyl derivatives. The reaction of acetylferrocene (**2a**), with an excess of triethyl orthoformate is reported to give a 48% yield of 1,3,5-triferrocenylbenzene (**1a**), and no 1,2,4-isomer after

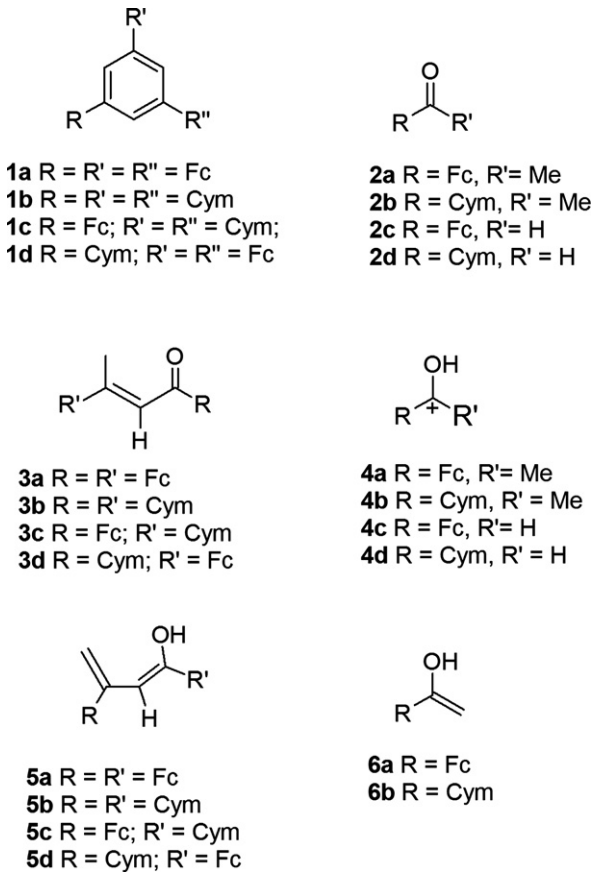

Chart 1.

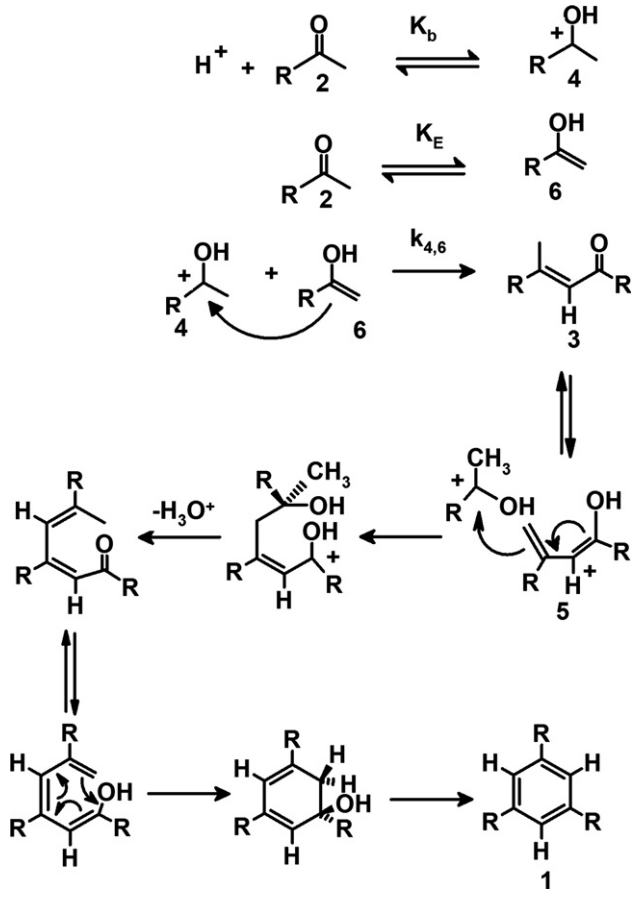

Scheme 1.

4 h [15]. A contradictory report [16] claimed that the same method produced large quantities of 1,3-diferrocenylbut-2-en-1-one (**3a**), and only trace amounts of **1a**. Compound **3a** has also been obtained from acetylferrocene by base-catalysis with lithium diisopropylamide (LDA) followed by work-up in dilute HCl [17]. We have previously shown that a mixture of $SiCl_4$–EtOH catalyzes the self-condensation of acetylferrocene and acetylcymantrene, reproducibly leading to the formation of the respective homo-metallic enone and aromatic structures **3a**,**b** and **1a**,**b** [18]. The present report examines the influence of stoichiometry on the product selection for the simultaneous cyclo-condensation of acetylferrocene (**2a**), and acetylcymantrene (**2b**). The heterometallic products were isolated, identified and characterized, and the factors that govern the formation of the products are discussed in light of the experimental evidence.

2. Experimental

2.1. Materials and methods

The manipulation of all organometallic reagents was performed under an atmosphere of dry nitrogen. Organic solvents were dried and distilled using standard procedures and stored over activated molecular sieves prior to use. Acetylferrocene, silicon tetrachloride and cymantrene were obtained from either Aldrich or Strem and used as received. Acetylcymantrene was prepared as described elsewhere [19]. Silica gel for column chromatography had a particle size of 20–45 μm.

Parallel syntheses were performed using a First-Mate Benchtop Synthesizer (Argonaut Technologies). HPLC analytical and semipreparative runs were performed at room temperature on a Waters Spherisorb 5 μm ODS2 analytical column (4.6 × 150 mm, flow rate 2 mL min^{-1}) or a Waters Spherisorb S5 ODS2 semipreparative column (10 × 250 mm, flow rate 9.5 mL min^{-1}) using the Waters 600E Multisolvent Delivery System (Waters 600 Controller, Waters 600E Pump). The separation was monitored with a Waters 2996 Photodiode Array Detector in conjunction with the Empower control software. Eluted fractions were delivered to a Waters Fraction Collector II and recovered with an Eppendorf 5301 Centrifugal Concentrator.

^1H and ^{13}C NMR spectra were acquired on Bruker AC 600, AC 500 or AC 200 spectrometers; chemical shifts are reported with respect to TMS and were determined by reference to the resonances of the residual proton or the natural abundance ^{13}C of the solvent. Direct electron impact (DEI) mass spectra were obtained with a Finnigan 4500 spectrometer. Infrared spectra were recorded on a Bio-Rad FTS-40 spectrometer as KBr pellets. Ultraviolet–visible spectra were recorded on a Cary 300 ultraviolet–visible spectrophotometer. Melting points were recorded uncorrected on a Thomas-Hoover melting point apparatus.

2.2. Preparative scale reaction of acetylferrocene (*2a*) with acetylcymantrene (*2b*)

In a typical experiment, a fresh solution of silicon tetrachloride in ethanol (30% v/v) was prepared under nitrogen by slow addition of the chloride to anhydrous solvent while stirring and maintaining room temperature. Once the evolution of HCl(g) ended, 0.5 mL of this solution was added to a solution consisting of acetylcymantrene (107.7 mg, 0.438 mmol) and acetylferrocene (99.9 mg, 0.438 mmol) in 1 mL of ethanol. The mixture developed a dark coloration and was gently stirred at room temperature. To stop the reaction after 72 h, 5 mL of an aqueous solution of sodium bicarbonate (10% w/v) were slowly added, and NaCl formed at the bottom of the tube. The organic components were extracted with dichloromethane (3 × 5 mL), dried with Na_2SO_4, and the solution was evaporated to dryness. The residue was redissolved in acetonitrile–water (80%, v/v) and separated using semi-preparative HPLC, using 100 μL portions at a time, with a stepwise elution gradient that began isocratic 85% v/v for 1.5 min, changed to 95% v/v acetonitrile–water with a linear gradient over 2.84 min, and remain isocratic until a total of 11 min had elapsed. Individual fractions were collected to recover the products, which were in order of elution:

(i) Unreacted acetylcymantrene $(CH_3C(O)C_5H_4)Mn(CO)_3$ (**2b**), t_r= 1.68 min.

(ii) Unreacted acetylferrocene $(CH_3C(O)C_5H_4)Fe(C_5H_5)$ **(2a)**, t_r = 1.75 min.

(iii) (*E*)-1,3-dicymantrenyl-2-buten-1-one, $RC(O)CH{=}C(CH_3)R$ [R = R′ = $(C_5H_4)Mn(CO)_3$] (**3b**) [18], t_r = 2.60 min.

(iv) (*E*)-3-cymantrenyl-1-ferrocenyl-2-buten-1-one, $RC(O)CH{=}C(CH_3)R'$ [R = $(C_5H_4)Fe(C_5H_5)$, R′ = $(C_5H_4)Mn(CO)_3$] (**3c**), t_r = 2.86. Yield: 73 mg (0.16 mmol, 35%). After solvent evaporation, the residue afforded dark red crystals from dichloromethane, m.p. 100–103 °C. IR (KBr) (cm^{-1}): 2031, 1916 (ν_{CO}), 1635 ($\nu_{C=O}$), 1579 ($\nu_{C=C}$). ^1H NMR (500 MHz, $CDCl_3$)δ: 6.75 (s, 1H), 5.26 (s, 2H), 4.88 (s, 2H), 4.80 (s, 2H), 4.55 (s, 2H), 4.22 (s, 5H), 2.37 (s, 3H). ^{13}C NMR (125 MHz, $CDCl_3$)δ: 224.2 (Mn–CO's), 194.1 (C=O), 144.3 (=C–CH_3), 120.7 (=CH), 101.6 (R-CpMn, C), 82.7, 82.6 (R-CpMn, CH's), 81.6 (R-CpFe, C), 72.5, 69.5 (R-CpFe, CH's), 69.9 (CpFe), 17.26 (CH_3). LR-MS (DEI) *m/z* (%): 456 ($[M]^+$, 50), 372 ($[M-3CO]^+$, 100), 318 (75), 252 (45), 213 ($[CpFe(C_5H_4)(CO)]^+$, 60), 185 ($[CpFe(C_5H_4)]^+$, 30), 149 (70), 129 (30), 120 ($[Fe(C_5H_4)]^+$, 10).

(v) 1-Cymantrenyl-3-ferrocenyl-2-buten-1-one [R = $(C_5H_4)Mn(CO)_3$, R′ = $(C_5H_4)Fe(C_5H_5)$] (**3d**), t_r = 3.35 min. Yield: 54 mg (0.12 mmol, 26%). After solvent evaporation the product was obtained as a red powder, m.p. 79–82 °C. IR (KBr) (cm^{-1}): 2020, 1934 (ν_{CO}), 1645 ($\nu_{C=O}$), 1586 ($\nu_{C=C}$). ^1H NMR (600 MHz $CDCl_3$)δ: 6.56 (s, 1H), 5.49 (s, 2H), 4.84 (s, 2H), 4.63 (s, 2H), 4.48(s, 2H), 4.17 (s, 5H), 2.53 (3H's). 13C NMR (125 MHz, $CDCl_3$)δ: 223.6 (Mn–CO's), 186.3 (C=O), 159.1 (R-CpMn, C), 115.2 (=CH), 97.3 (=C–CH_3), 86.4, (R-CpMn, CH's),

85.2 (R-CpFe, C), 83.5 (R-CpMn, CH's), 71.3 (R-CpFe, CH's), 70.1 (CpFe), 67.5 (R-CpFe, CH's), 18.6 (CH_3). LR-MS (DEI) *m/z* (%): 456 ($[M]^+$, 50), 429 (25), 372 ($[M-3CO]^+$, 100), 355 (25), 305 (20), 252 (20), 228 (50), 185 ($[CpFe(C_5H_4)]^+$, 50), 149 (30), 129 (35).

(vi) (*E*)-1,3-diferrocenyl-2-buten-1-one, $RC(O)CH{=}C(CH_3)R$ [$R = R' = (C_5H_4)Fe(C_5H_5)$] (**3a**) [15], t_r = 3.56 min.

(vii) 1,3,5-Tricymantrenylbenzene, 1,3,5-$R_3C_6H_3$ [$R = (C_5H_4)Mn(CO)_3$] (**1b**) [18], $t_r = 4.86$ min.

(viii) 1,3-Dicymantrenyl-5-ferrocenylbenzene, 1,3,5-$R_2R'C_6H_3$ [$R = (C_5H_4)Mn(CO)_3$, $R' = (C_5H_4)Fe(C_5H_5)$] (**1c**), $t_r = 6.59$ min. After solvent evaporation the product was isolated as a yellow-brown powder, m.p. 180–184 °C. IR (KBr) (cm^{-1}): 2020, 1932 (ν_{CO}). ^1H NMR (500 MHz, CD_2Cl_2) δ: 7.44 (s, 2H), 7.28 (s, 1H), 5.33 (s, 4H), 4.89 (s, 4H), 4.72 (s, 2H), 4.38 (s, 2H), 4.07 (s, 5H). ^{13}C NMR (125 MHz, CD_2Cl_2)δ: 225.6 (Mn–CO's), 134.2, 124.1 (Aryl, CH), 121.9, 103.2 (Aryl, C), 84.2 (R-CpMn, C), 83.3 (R-CpFe, C), 83.2, 82.3 (R-CpMn, CH's), 70.3 (CpFe), 70.0, 67.2 (R-CpFe, CH's). LR-MS (DEI) *m/z* (%): 666 ($[M]^+$, 60), 582 ($[M-3CO]^+$, 55), 498 ($[M-6CO]^+$, 100), 443 (60), 388 (10), 265 (8), 249 (15), 121 ($[Fe(C_5H_5)]^+$, 3), 55 ($[Mn]^+$, 5).

(ix) 1-Cymantrenyl-3,5-diferrocenylbenzene, 1,3,5-R_2R'-C_6H_3 [$R = (C_5H_4)Fe(C_5H_5)$ $R' = (C_5H_4)Mn(CO)_3$] (**1d**), $t_r = 8.24$ min. After solvent evaporation the residue afforded orange crystals from dichloromethane, m.p. 201–203 °C. IR (KBr) (cm^{-1}): 2016, 1932 (ν_{CO}). ^1H NMR (500 MHz, CD_2Cl_2) δ: 7.53 (s, 1H), 7.36 (s, 2H), 5.35 (s, 2H), 4.90 (s, 2H), 4.74 (s, 4H), 4.38 (s, 4H), 4.09 (s, 10H). ^{13}C NMR (125 MHz, CD_2Cl_2)δ: 225.8 (Mn-CO's), 140.6 (Aryl, CH), 133.5, 124.2 (Aryl, C), 122.0 (Aryl, CH), 104.2 (R-CpMn, C), 85.2, 83.2 (R-CpMn, CH's), 82.0 (R-CpFe, C), 70.3 (CpFe), 69.8, 67.2 (R-CpFe, CH's). LR-MS (DEI) *m/z* (%): 648 ($[M]^+$, 100), 564 ($[M-3CO]^+$, 90), 510 ($[M-Mn(CO)_3]^+$, 100), 121 ($[Fe(C_5H_5)]^+$, 89), 69 (15).

(x) 1,3,5-Triferrocenylbenzene, 1,3,5-$R_3C_6H_3$ [(C_5H_4)-$Fe(C_5H_5)$] (**1a**) [14], t_r. = 10.13 min.

N.B. The fractions separated by HPLC were stable and always afforded a single peak each when reinjected into the HPLC. However, the amount of each heterometallic compound recovered even after repeated runs was too small to permit reliable combustion elemental analyses.

2.3. Quantitative determination of yields

Stock solutions of the organometallic reagents were prepared by dissolving **2a** (1.997 g, 8.76 mmol) and **2b** (2.150 g, 8.76 mmol) each in 10 mL dichloromethane. These stock solutions were used to prepare mixtures with **2a/2b** molar ratios 2:1 (0.067 g, 0.1440 g), 1:1 (0.0999 g, 0.1077 g) and 1:2 (0.133 g, 0.072 g); a control solution contained no reactant and was handled in exactly the same manner as the others. Each mixture was concentrated to form a pellet in the centrifugal concentrator and re-dissolved in dry ethanol (1 mL) under nitrogen in the parallel reactor. The solutions were then mixed with 0.5 mL a freshly prepared mixture of $SiCl_4$ in ethanol (30% v/v) and allowed to react at room temperature. The mixtures were treated with a 10% aqueous solution of $NaHCO_3$ (5 mL) and extracted using of dichloromethane (2.5 mL); 1 mL of each organic extract was dried using Na_2SO_4, filtered and concentrated to a pellet. These residues were re-dissolved in an appropriate amount of an acetonitrile–water mixture and passed through an analytical C-18 column using an optimized elution profile beginning with 85% v/v acetonitrile–water for 2.5 min, changing linearly to 95% v/v acetonitrile in 1.7 min and keeping the mobile phase composition through the end of the run. Separate experiments were conducted after 72 and 14 h of reaction time.

2.4. Measurement of pK_a values

In order to determine the basicity of **2a** and **2b** by Hammett's procedure [20], weighed samples of the ketones were dissolved in mixtures of ethanol/sulfuric acid of known composition, and their ultraviolet visible spectra were recorded with individual baseline corrections for each solvent composition.

2.5. X-ray crystallography

Single crystals of **1d** and **3c** were grown via slow evaporation in a methylene chloride–hexane mixture and mounted on a glass fiber using epoxy resin. X-ray diffraction data sets were collected on a P4 Bruker diffractometer upgraded with a Bruker SMART 1000 CCD detector and a rotating anode utilizing Mo Kα radiation ($\lambda = 0.7103$ Å, graphite monochromator) equipped with an Oxford cryosystem. For each compound, a full sphere of reciprocal lattice was scanned by 0.36° steps in θ with a crystal-to-detector distance of 4.9 cm. Preliminary orientation matrices were obtained from the first frames using SMART [21]. The collected frames were integrated using the preliminary orientation matrices which were updated every 100 frames. Final cell parameters were obtained by refinement on the positions of reflections with $I > 10s(I)$ after integration of all the frames using SAINT [21]. The data sets were empirically corrected for absorption and other effects using SADABS [22]. The structures were solved by direct methods and refined by full-matrix least squares on all F^2 data using SHELXTL [23]. The non-H atoms were refined anisotropically, while H atoms were constrained to idealized positions using appropriate riding models. Molecular graphics were produced using ORTEP-3 and POVRAY [24].

2.6. Computational methods

The optimization of structures were performed using the ADF DFT package (version 2006.01) [25]. The Adiabatic Local density Approximation (ALDA) was used for the

exchange-correlation kernel [26] and the differentiated static LDA expressions were used with the Vosko–Wilk–Nusair parametrization [27]. The optimization of model geometries was gradient-corrected with the exchange and correlated functionals of the gradient correction proposed in 1988 by Becke [28] and Perdew [29]. Preliminary geometry optimizations were conducted using a double-ζ basis set with frozen cores corresponding to the configuration of the preceding noble gas with polarization functions; the resulting structures were refined using a triple-ζ all-electron basis set with one polarization function. Electronic excitations were calculated using time-dependent density functional theory (TDDFT) as implemented within the ADF package; the Statistical Average of different model Potentials for occupied KS Orbitals (SAOP) [30] was used for the exchange-correlation potentials in the zeroth-order KS equations.

3. Results and discussion

3.1. Synthesis and purification of the products of condensation

Individual ethanolic solutions of the acetyl-substituted cyclopentadienyl metal complexes **2a** and **2b** readily reacted upon addition of $SiCl_4$ (10% v/v). The ferrocenyl derivative, **2a**, afforded a red solution while the cymantrenyl ketone, **2b**, developed a violet coloration. Upon standing for 72 h at room temperature, these conditions produced the corresponding 1,3,5-homosubstituted benzenes (**1a**, 73%; **1b**, 16%) and the intermediate enone condensation products (**3**a, 26%; **3b**, 79%). In both instances, the yields were readily determined by ^{1}H NMR and the products were conveniently separated from the intermediates and the residual starting materials using column chromatography. On the other hand, mixtures of **2a** and **2b** should yield four different cyclo-condensation products **1a**–**1d**, and four intermediates **3a**–**3d**, neglecting the possibility of formation of larger molecules [31,32]. In preliminary experiments the ^{1}H NMR spectra were too complicated to be conclusively interpreted, even at 600 MHz. Since it was also very difficult to separate all four compounds of type **3** by means of simple column chromatography, it was necessary to use HPLC to purify and quantify the products. In an earlier publication Štěpnička and co-workers [33] reported an HPLC method for the analytical separation of 1,3,5-triferrocenylbenzene (**1a**), and the isomeric 1,2,4-triferrocenylbenzene at room temperature on a 40×250 mm LiChrospher WP 300 (Merck) reverse-phase column with a 1 cm^3 min^{-1} flow rate for a linear gradient elution from 1:1 acetonitrile:water to 100% acetonitrile over 120 min. In the present case, these conditions were adapted for a 4.6×150 mm Spherisorb 5 μm ODS2 (Waters) analytical column but extensive overlap of peaks was observed in the chromatogram recorded at 254 nm. The separation was optimized following standard procedures [34]; the customized method consisted of an isocratic-gradient-isocratic stepwise elution profile. The flow rate was constant at 2 mL min^{-1}, and the separation was best monitored at 285 nm. These conditions led to short retention times while achieving a minimum peak resolution of 0.92; a typical separation result is presented in Fig. 1. The identity of each species was established first by comparison of the retention time for actual samples of the known homometallic compounds: **2a**, **2b**, **3a**, **3b**, **1a** and **1b**. In order to assign the remaining bands the separation was scaled up using a larger column pack with the same stationary phase, the relevant bands were collected several times, the solvent was removed and the residues were characterized as described below. Four main regions were then identified in the chromatogram. The first ($t < 2$ min) includes the bands of the two acetyl starting materials **2a** and **2b**; the second (2 min $< t <$ 4 min) contains the bands of the four enone intermediate products of condensation, **3**; the last region ($t > 4$ min) contains the bands of the four 1,3,5-substituted benzenes. Overall, and within each region,

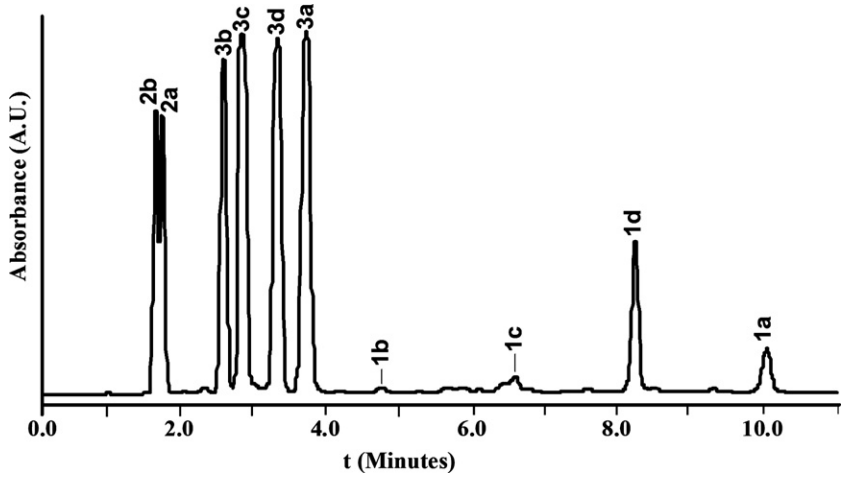

Fig. 1. An analytical-scale chromatogram for a 1:1 reaction mixture of **2a** and **2b** after 72 h. The identities of the products were established by comparison to actual samples, and also by ^{1}H NMR spectroscopy and X-ray crystallography.

the order of elution reflects the polarity of all the species, which decreases as the molecules increase in size, and as the number of ferrocenyl groups increases. Although larger oligomeric products [31,32] have been observed in related syntheses, no additional bands were observed when the runs were prolonged for an additional 30 min under constant eluent composition.

3.2. Spectroscopic identification of *1c, 1d, 3c* and *3d*

The identity of these species was established in first instance by mass spectrometry, whereby all spectra displayed the $[M]^+$ ion, and was confirmed by NMR spectroscopy. The plane of symmetry inherent to both mixed-metal tri-substituted benzenes **1c** and **1d** leads to ^{13}C NMR spectra that contain the same number and type of signals. More informative are the ^1H NMR spectra: while the spectrum of compound **1c** is characterized by integration ratios 1:2:4:4:2:2:5 that of **1d** displays ratios 1:2:2:2:4:4:10 reflecting the number of ferrocenyl and cymantrenyl substituents on the aromatic ring. In contrast, the mixed-metal enones **3c** and **3d** are structural isomers and cannot be distinguished unequivocally by simple 1D ^1H or ^{13}C NMR spectroscopy; moreover, the mass spectra provided no useful fragments. Consequently, the identification of these compounds was secured by using X-ray crystallography to determine the structure of **3c**. Despite the size of the ferrocenyl and cymantrenyl substituents, variable-temperature NMR provided no evidence of slow rotation in any of **3a**, **3b**, **1a** and **1b**.

3.3. X-ray crystallography

In addition to the iron-manganese enone, **3c**, the mixed-metal trisubstituted arenes ($FeMn_2$) (**1c**), and (Fe_2Mn) (**1d**), were also characterized crystallographically. The refinement data for **1d** and **3c** are summarized in Table 1, and selected bond distances and angles are given in Table 2. The crystal of **1d** was determined to be twinned by a two-fold rotation around the 1,0,0 direct lattice direction and detwinned by applying the appropriate rotation matrix. After the final structure was solved, the fraction of the minor component was determined to be 40.803%. The structure of **1d** (Fig. 2) features a "two-up, one-down" arrangement of the organometallic groups, reminiscent of the solid-state structures of the tri-iron and tri-manganese analogues, **1a** and **1b**, respectively [18,33]. The asymmetric unit in the crystal structure of the $MnFe_2$ complex, **1d**, contains only one molecule, and all bond distances and bond angles do not differ significantly from the corresponding values in the tri-iron species, **1a**. The same geometric arrangement was evident from analysis of preliminary diffraction data of a single crystal the Mn_2Fe complex, **1c**, but a combination of severe substitutional and positional disorders of one ferrocenyl and one of the cymantrenyl groups precluded a satisfactory refinement of the structure. On the other hand, the Fe–Mn enone **3c** (Fig. 3), adopts the *E* form in the solid-state, very similar to the structure of its homo-ferrocenyl dimer counterpart, **3a** [17]. The average C–C bond length (1.417(3) Å) for the unsubstituted cyclopentadienyl ring of the ferrocenyl group is comparable to the corresponding values in the substituted cyclopentadienyl rings in the ferrocenyl and cymantrenyl systems, (1.428(2) Å and 1.423(2) Å, respectively). The C=C double-bond distance ([1.342(2) Å) is within the range

Table 1
Summary of crystal data, collection and refinement conditions for **1d** and **3c**

	1d	**3c**
Formula	$C_{34}H_{25}Fe_2MnO_3$	$C_{22}H_{17}FeMnO_4$
Formula weight	648.18	456.15
Radiation (wavelength, Å)	0.71073	0.71073
Temperature	173(2)	173(2)
Crystal system	Monoclinic	Monoclinic
Space group	$P2_1/c$	$P2_1/c$
a (Å)	12.377(4)	17.895(5)
b (Å)	19.440(7)	9.291(3)
c (Å)	12.507(4)	11.426(3)
α (°)	90.00	90.00
β (°)	119.535(5)	98.563(9)
γ (°)	90.00	90.00
Volume (Å^3)	2618.3(16)	1878.5(9)
Z	4	4
$\delta_{calcd.}$(g/cm^3)	1.644	1.613
μ (mm^{-1})	1.605	1.470
R_1^a	0.051	0.047
wR_2^b	0.103	0.081

[a] $R_1 = \sum ||F_o| - |F_c|| / \sum |F_o|$.
[b] $wR_2 = (\sum w||F_o| - |F_c||^2 / \sum w|F_o|^2)^{1/2}$.

Table 2
Selected bond lengths (Å), bond angles (°) and inter-planar angles (°) for **1d** and **3c**

1d		**3c**	
Average distances			
C–C (Aryl)	1.393(8)	C–C(Fc, Cp)	1.421(3)
C–C (Fc, Cp)	1.42(1)	C–C(Cym, Cp)	1.423(2)
C–C (Cym, Cp)	1.421(9)	Fe–C	2.044(2)
Fe–C	2.037(7)	Mn–C(Cp)	2.144(2)
Mn–C (Cp)	2.144(7)	Mn–CO	1.796(2)
Mn–CO	1.782(7)	C_2–C_3	1.342(2)
Distances			
C_2–C_{31}	1.475(8)	C_1–C_2	1.479(2)
C_4–C_{11}	1.481(8)	C_1–C_{21}	1.468(2)
C_6–C_{21}	1.483(8)	C_3–C_{11}	1.480(2)
Bond angles			
C_1–C_2–C_3	119.4(6)	C_1–C_2–C_3	126.5(1)
C_1–C_2–C_{31}	119.6(5)	C_2–C_3–C_{11}	119.7(1)
C_2–C_3–C_4	120.4(6)	C_3–C_{11}–C_{15}	127.0(2)
C_3–C_4–C_5	119.1(5)	C_1–C_{21}–C_{22}	130.8(1)
Inter-planar angles			
Plane	Angles	Plane	Angles
1 C_1–C_6		1 C_1–C_4	
2 C_{11}–C_{15}	1,2 = 5.8(4)	2 C_{11}– C_{15}	1,2 = 13.05(8)
3 C_{21}–C_{25}	1,3 = 20.2(4)	3 C_{21}–C_{25}	1,3 = 5.72(8)
4 C_{31}–C_{35}	1,4 = 13.4(4)		

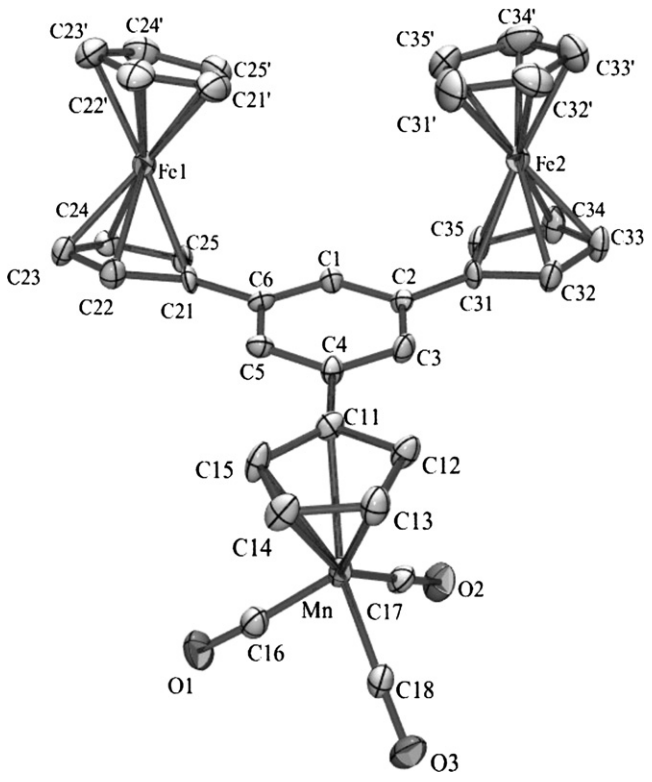

Fig. 2. The ORTEP diagram of 1-cymantrenyl-3,5-ferrocenylbenzene (**1d**) (50% thermal ellipsoids; the hydrogen atoms are omitted for clarity).

(1.343(4)–1.392(3) Å) observed for C=C double bonds in compounds of similar structure, such as enolized asymmetric 1,3-diketones [35].

3.4. Yields

Although the generalities of the overall reaction are established, there is some disagreement on the precise nature of all the intermediates formed during the process of cyclo-condensation of ketones induced by $SiCl_4$ in alcoholic media. It has been proposed that $SiCl_4$ functions as a ketalizing agent [17], other reports advocate a mechanism which includes partial solvolysis of $SiCl_4$ to form species of composition $Cl_xSi(OEt)_{4-x}$ [36]. For simplicity, the latter scenario was assumed, which implies that the mixture of $SiCl_4$ and EtOH behaves as a steady, if not controlled, source of anhydrous HCl. The mechanism shown in Scheme 1 is directly applicable to this case. According to this sequence, all the enone intermediates of type **3** have in principle an equal chance to be formed by one channel each, whereby an enol reacts with a protonated ketone:

6a + **4a** → **3a** (1a)

6a + **4b** → **3c** (1c)

6b + **4a** → **3d** (1d)

6b + **4b** → **3b** (1e)

While the benzenes are obtained by eight channels, six which favor the formation of the heterometallic molecules by reaction of **3** (via its enolized form **5**) with **4**:

3a + **4a** → **1a** (2a)

3a + **4b** → **1d** (2b)

3b + **4a** → **1c** (2c)

3b + **4b** → **1d** (2d)

3c + **4a** → **1d** (2e)

3c + **4b** → **1c** (2f)

3d + **4a** → **1d** (2g)

3d + **4b** → **1c** (2h)

However, the cyclocondensation of a mixture of **2a** and **2b** would only produce a statistical distribution of products if all the intermediates are formed and consumed at rates that are independent of the nature of their pendant func-

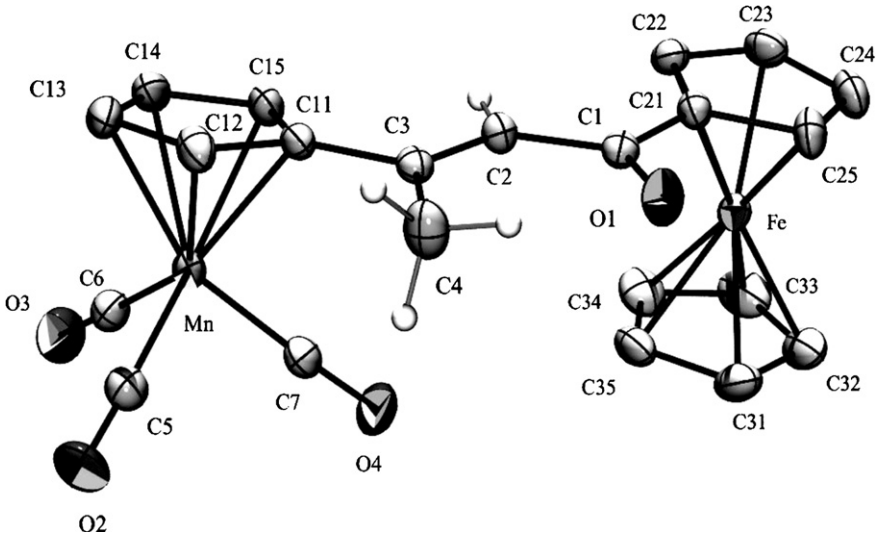

Fig. 3. The ORTEP diagram of (*E*)-3-cymantrenyl-1-ferrocenyl-2-buten-1-one (**3c**) (50% thermal ellipsoids; the hydrogen atoms (except those on the methyl group) are omitted for clarity).

tional groups. However, some of these intermediates are formally carbocations, whose stability is readily influenced by adjacent organometallic substituents, ferrrocenyl and cymantrenyl in the present case.

The yields of the condensation products for different **2a**:**2b** ratios were measured using the HPLC method developed for purification at analytical scale, with appropriate calibration curves for each component of the mixture. Reactions with three different initial compositions were run in parallel to minimize possible variations of the conditions on each trial, chiefly the acidity of the medium since the $SiCl_4$/EtOH mixture releases HCl over time. Under the conditions of the experiment, the reaction is slow and the formation of the benzenes can only be reliably quantified after 48 h. Table 3 presents the yields of heterometallic 1,3,5-trisubstituted benzenes. It is remarkable that for all three mixtures there is a bias for the formation of the molecule with two ferrocenyl groups, **1d**. This could be attributable either to the preferential formation of **3a** in the early stages of the reaction, or the predominance of the reaction of the protonated **4a** with the heterometallic species **3c** and **3d**. In order to investigate these hypotheses, the reactions were repeated and stopped at an earlier stage, 14 h after addition of the catalyst. The results of the analysis for the yields of all compounds of type **3** are presented in Table 3. At this time the benzenes could not be detected and the hetero-substituted compounds **3c** and **3d** form preferentially over their homo-metallic counterparts. Interestingly, the yield of **3c** is consistently lower than that of **3d**, an observation which provides further insight into the factors that control the reaction, as shown below.

Since thermodynamics favors formation of the benzenes, formation of the intermediate complexes **3** is under kinetic control. From Scheme 1, before any **1** is formed, the following rate law governs the concentration of each **3** in the early stages of the reaction:

$$d[\mathbf{3}]/dt = k_T[H^+][\mathbf{2}][\mathbf{2}] \quad (3)$$

where

$$k_T = K_{b2}K_{E2}k_{4,6} = (K_i/K_{a2})K_{E2}k_{4,6} \quad (4)$$

From this, the rate constant k_T depends on three parameters which include: the protonation equilibrium constant (K_b) and the tautomerization equilibrium constant (K_E) of the respective reactants **2**, and the rate constant ($k_{4,6}$) for the addition of the enol **6** to the protonated species **4**. This expression can also be written in terms of the acidity constant, K_a, of species **4** and the auto-ionization constant, K_i, of ethanol. This formulation of the rate constant can be used to interpret the experimentally observed amounts of the mixed-metal α,β-unsaturated ketones. Comparison of the relative abundances of **3c** to that of **3d** suggests that:

$$(K_i/K_{a4b})K_{E2a}k_{4b,6a} < (K_i/K_{a4a})K_{E2b}k_{4a,6b} \quad (5)$$

It is reasonable to expect that K_E and $k_{4,6}$ would have similar values for each ketone (**2a** and **2b**), and therefore the different amounts of the intermediates **3** are mostly related to the difference of K_a between **2a** and **2b**.

Table 3
The relative yield of the products **1c–1d** after 48 h, and of the intermediates **3a–3d** after 14 h as a function of the relative amounts of the reactants **2a** and **2b**

Initial molar fractions of reactants		Yield (% molar)					
		48 h		14 h			
2a	**2b**	**1c**	**1d**	**3a**	**3b**	**3c**	**3d**
0.33	0.67	3.6	10	3.1	11	29	36
0.50	0.50	2.7	20	9.9	4.6	30	40
0.67	0.33	2.5	20	22	1.5	26	34

3.5. Basicities of *2a* and *2b*

The striking color changes observed in solutions of **2a** and **2b** immediately upon addition of the catalyst suggested that these could be, in first instance, the result of protonation to form the intermediates **4**. Figs. 4 and 5

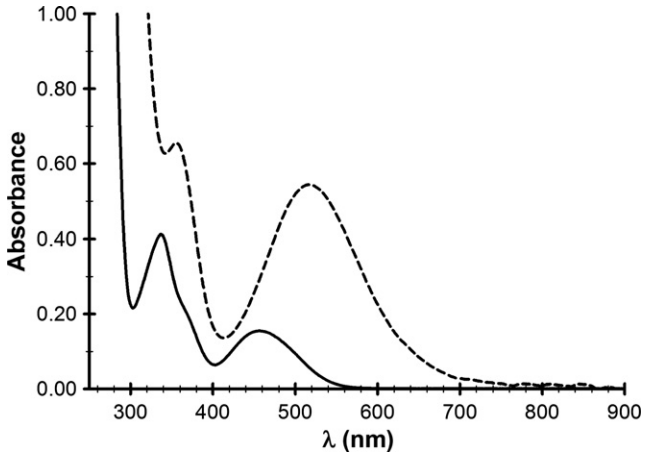

Fig. 4. Ultraviolet–visible absorption spectra of **2a**, 10.8 mmol/L, in 0% (—) and 60% (––) (v/v) H_2SO_4 in ethanol.

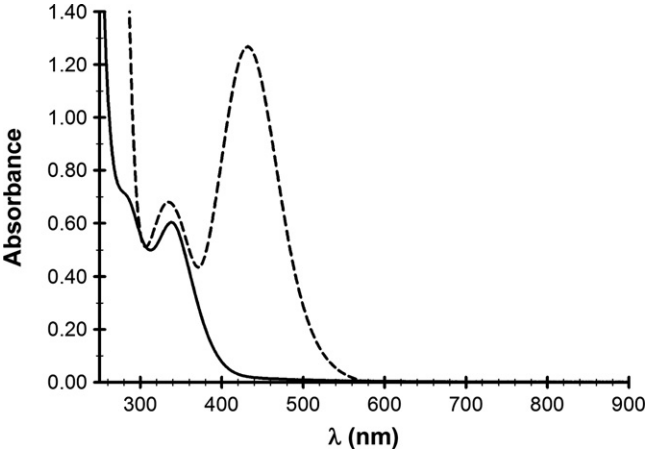

Fig. 5. Ultraviolet–visible absorption spectra of **2b**, 11.2 mmol/L, in 0% (—) and 80% (––) (v/v) H_2SO_4 in ethanol.

compare the UV–visible spectra of dilute solutions of the acetyl-cyclopentadienyl complexes **2a** and **2b**, respectively, in neutral and strongly acidic media. In each case, the spectrum of the protonated species is characterized by an increase of absorbance at long wavelengths. The assignment of these spectra to the protonated species of the type **4** was aided by TD-DFT calculations of the electronic excitations of the optimized model compounds **2c**, **2d**, **4c** and **4d**. The results of these calculations mimicked well the main features of experimental spectra. In all cases, the most intense band at long wavelength originates in a charge transfer from d orbitals into an antibonding orbital of the ligand that has a large contribution from the carbon atom of the carbonyl; hence this excitation is very sensitive to protonation of the oxygen atom. Fig. 6 displays the transition density of these transitions, which is calculated as the product of the ground and excited states:

$$\rho_{ge}(\mathbf{r}) = \psi_g^*(\mathbf{r})\psi_e(\mathbf{r}) \quad (6)$$

This enabled determination of the pK_a's of **4a** and **4b** with a spectrophotometric titration based on the Hammett acidity function [20]:

$$\log([BH+]/[B]) = pK_a - H_0(\%H_2SO_4) \quad (7)$$

Fig. 7 presents plots of the acidity function at different concentrations of sulfuric acid. The values of pK_a extracted from these experiments are −2.6 for **2a** and −4.0 for **2b**. Both compounds are more basic than common organic carbonyl compounds, which have pK_a values that range from −6.99 (benzaldehyde) to −6.04 (acetophenone) [37], but acetylferrocene is a stronger base than acetylcymantrene. The difference of more than one order of magnitude in pK_a indicates that the ferrocenyl group is much more efficient at stabilizing the formal carbocation of type **4**. This is consistent with the $\Delta H = 55$ kJ/mol for the hypothetical reaction (8) estimated from the total bonding energies calculated by DFT

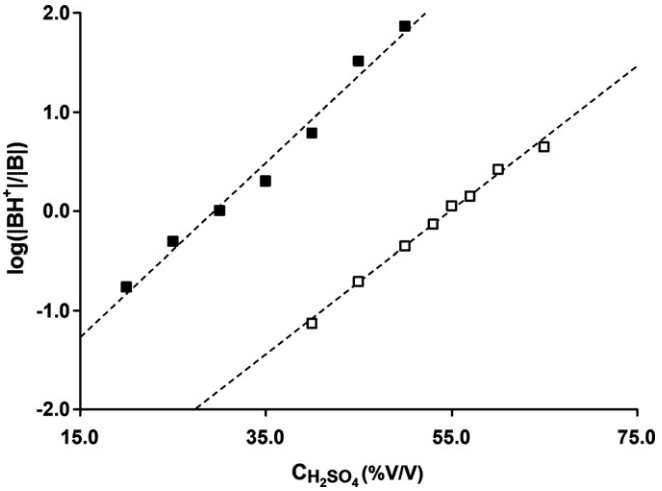

Fig. 7. Hammett acidity function plots for the measurement of the pK_a values in ethanol of **2a** (■) and 2b (□).

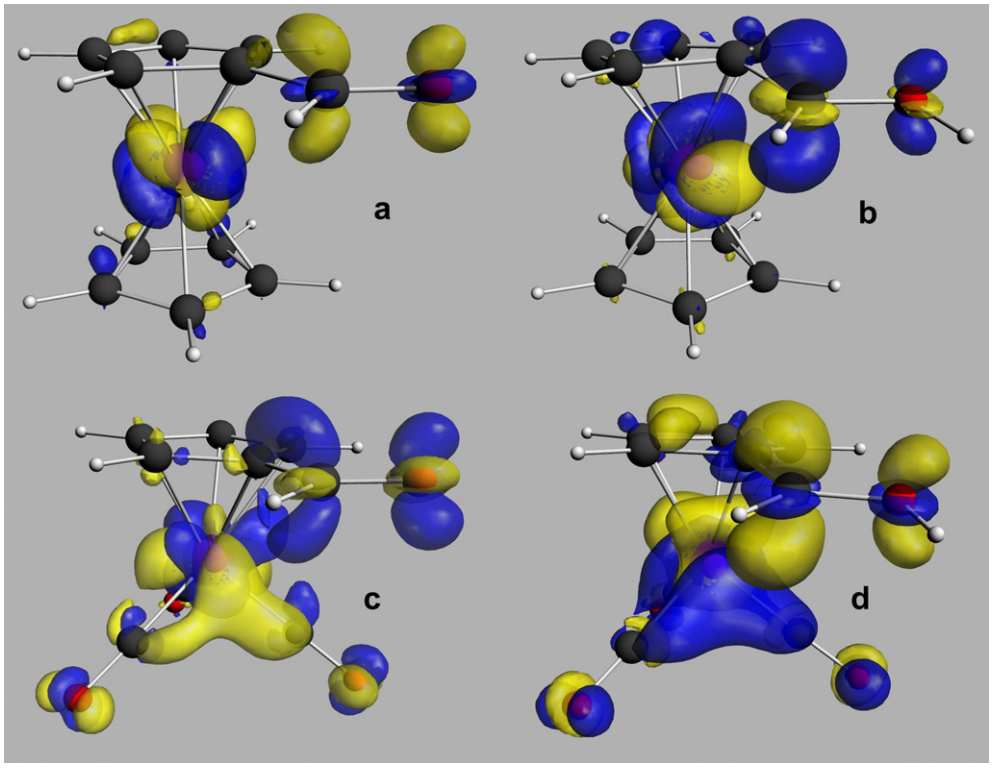

Fig. 6. Transition density plots for the first intense electronic excitation of (a) **2c**, (b) **2d**, (c) **4c**, and (d) **4d**. Yellow and blue represent in-phase and out-of-phase lobes, respectively.

$$\mathbf{2a} + \mathbf{4b} \rightarrow \mathbf{4a} + \mathbf{2b} \quad (8)$$

In consequence, the medium in the cyclocondensation reaction is richer in **4a** than **4b**. This factor explains not only the preferential formation of **3d** over **3c** by reaction with the cymantrenylenol, but it is consistent with the overall abundance of **1d** formed in the subsequent reaction of the tautomerized **3d** with **4a**.

4. Conclusion

Under the conditions of this study, the cyclo-condensation of acetylferrocene and acetylcymantrene in $SiCl_4$-ethanol mixtures has been shown to yield predominantly heterometallic 1,3,5-substituted benzenes and significant amounts of 1,3-disubstituted-2-buten-1-ones. Four new heterometallic compounds that contain both ferrocenyl and cymantrenyl substituents, namely (*E*)-3-cymantrenyl-1-ferrocenyl-2-buten-1-one (**3c**), (*E*)-1-cymantrenyl-3-ferrocenyl-2-buten-1-one (**3d**), 1,3-dicymantrenyl-5-ferrocenylbenzene (**1c**) and 1-cymantrenyl-3,5-diferrocenylbenzene (**1d**), in addition to their homometallic analogues, were prepared simultaneously. The relative yields of the different products are determined by the greater basicity of the ferrocenyl derivative, which forms larger amounts of the protonated intermediate; this in turn determines the structure of the most abundant intermediate and the final product. It is therefore not possible to select the final product by simply changing the stoichiometry of the reactants.

Acknowledgements

This project was supported by grants from the Natural Sciences and Engineering Research Council of Canada (NSERC), the Canada Foundation for Innovation (CFI), and the Ontario Innovation Trust (OIT). This work was made possible by the facilities of the Shared Hierarchical Academic Research Computing Network (SHARCNET: www.sharcnet.ca).

Appendix A. Supplementary material

CCDC 677373 and 677372 contain the supplementary crystallographic data for this paper. These data can be obtained free of charge from The Cambridge Crystallographic Data Centre via www.ccdc.cam.ac.uk/data_request/cif. Supplementary data associated with this article can be found, in the online version, at doi:10.1016/j.jorganchem.2008.02.013.

References

[1] (a) L. de Quadras, F. Hampel, J.A. Gladysz, Dalton Trans. (2006) 2929–2933;
(b) H. Fukumoto, K. Mashima, Eur. J. Inorg. Chem. (2006) 5006–5011;
(c) H. Fukumoto, K. Mashima, Organometallics 24 (2005) 3932–3938;
(d) W.-Y. Wong, Coord. Chem. Rev. 249 (2005) 971–997;
(e) J.-P. Launay, Chem. Soc. Rev. 30 (2001) 386–397;
(f) V.W.-W. Yam, Chem. Commun. (2001) 789–796;
(g) C. Joachim, J.K. Gimzewski, A. Aviram, Nature 408 (2000) 541–548;
(h) P. Nguyen, P. Gómez-Elipe, I. Manners, Chem. Rev. 99 (1999) 1515–1548;
(i) V.W.-W. Yam, K.K.-W. Lo, K.M.-C. Wong, J. Organomet. Chem. 578 (1999) 3–30;
(j) R. Ziessel, M. Hissler, A. El-Ghayoury, A. Harriman, Coord. Chem. Rev. 178–180 (1998) 1251–1298;
(k) F. Paul, C. Lapinte, Coord. Chem. Rev. 178–180 (1998) 431–509;
(l) J.T. Lin, M.-F. Yang, C. Tsai, Y.S. Wen, J. Organomet. Chem. 564 (1998) 257–266;
(m) D. Astruc, Acc. Chem. Res. 30 (1997) 383–391;
(n) S. Barlow, D. O'Hare, Chem. Rev. 97 (1997) 637–669;
(o) J.J. Irwin, M.J. Vittal, R.J. Puddephatt, Organometallics 16 (1997) 3541–3547;
(p) M.D. Ward, Chem. Soc. Rev. (1995) 121–134.
[2] (a) A. Caballero, A. Espinosa, A. Tárraga, P. Molina, J. Org. Chem. 72 (2007) 6924–6937;
(b) W.-Y. Wong, K.-Y. Ho, K.-H. Choi, J. Organomet. Chem. 670 (2003) 17–26.
[3] (a) B. Bildstein, Coord. Chem. Rev. 206–207 (2000) 369–394;
(b) W.-Y. Wong, W.-K.P. Wonga, R. Raithby, J. Chem. Soc., Dalton Trans. (1998) 2761–2766;
(c) D.R. Kanis, M.A. Ratner, T.J. Marks, J. Am. Chem. Soc. 114 (1992) 10338–10357.
[4] (a) H. Le Bozec, T. Le Bouder, O. Maury, I. Ledoux, J. Zyss, J. Opt. A 4 (2002) S189–S196;
(b) M. Cho, S.-Y. An, H. Lee, I. Ledoux, J. Zyss, J. Chem. Phys. 116 (2002) 9165–9173;
(c) C. Fiorini, F. Charra, J.-M. Nunzi, I.D.W. Samuel, J. Zyss, Opt. Lett. 20 (1995) 2469–2471;
(d) J. Zyss, C. Dhenaut, T. Chauvan, I. Ledoux, Chem. Phys. Lett. 206 (1993) 409–414;
(e) J. Zyss, V. Thai Chau, C. Dhenaut, I. Ledoux, Chem. Phys. 177 (1993) 281–296.
[5] (a) G. Hennrich, I. Asselberghs, K. Clays, A. Persoons, J. Org. Chem. 69 (2004) 5077–5081;
(b) J. Zyss, I. Ledoux-Rak, H.-C. Weiss, D. Blaeser, R. Boese, P.K. Thallapally, V.R. Thalladi, G.R. Desiraju, Chem. Mater. 15 (2003) 3063–3073;
(c) J. Brunel, O. Mongin, A. Jutand, I. Ledoux, J. Zyss, M. Blanchard-Desce, Chem. Mater. 15 (2003) 4139–4148;
(d) A.M. McDonagh, M.G. Humphrey, M. Samoc, B. Luther-Davies, S. Houbrechts, T. Wada, H. Sasabe, A. Persoons, J. Am. Chem. Soc. 121 (1999) 1405–1406;
(e) V.R. Thalladi, S. Brasselet, D. Blaser, R. Boese, J. Zyss, A. Nangia, G.R. Desiraju, Chem. Commun. (1997) 1841–1842;
(f) J.L. Bredas, F. Meyers, B.M. Pierce, J. Zyss, J. Am. Chem. Soc. 114 (1992) 4928–4929.
[6] K.P.C. Vollhardt, Acc. Chem. Res. 10 (1977) 1–8.
[7] (a) S.S. Elmorsy, A.G.M. Khalil, M.M. Girges, T.A. Salama, J. Chem. Res. (S) (1997) 232–233;
(b) M.J. Plater, J. Chem. Soc., Perkin Trans. 1 (1997) 2897–2901;
(c) S. Kotha, K. Chakraborty, E. Brahmachary, Synlett 10 (1999) 1621–1623.
[8] M.R. Buchmeiser, R.R. Schrock, Macromolecules 28 (1995) 6642–6649.
[9] (a) J. Yang, J.G. Verkade, J. Am. Chem. Soc. 120 (1998) 6834–6835;
(b) J. Yang, J.G. Verkade, Organometallics. 19 (2000) 893–900.
[10] H.O. Wirth, W. Kern, E. Schmitz, Makromol. Chem. 68 (1963) 69–99.
[11] (a) R.B.N. Ansems, L.T. Scott, J. Am. Chem. Soc. 122 (2000) 2719–2724;
(b) A.N. Pyrko, Zh. Org. Khim. 28 (1992) 215–216;
(c) R. Meyer, Chem. Ber. (1956) 1443–1454;

(d) R. Seka, W. Kellermann, Ber. Dtsch. Chem. Ges. 75 (1942) 1730–1738;
(e) O. Wallach, Chem. Ber. (1897) 1094–1096.
[12] (a) K. Shahlai, H. Hart, J. Am. Chem. Soc. 110 (1988) 7136–7140;
(b) K. Komatsu, S. Aonuma, Y. Jinbu, R. Tsuji, K. Takeuchi, J. Org. Chem. 56 (1991) 195–203;
(c) A.J. Barkovich, E.S. Strauss, K.P.C. Vollhardt, J. Am. Chem. Soc. 99 (1977) 8321–8322;
(d) D.S. Greidinger, D. Ginsburg, J. Org. Chem. 22 (1957) 1406–1410.
[13] N.O. Mahmoodi, M.K. Fatemeh, J. Korean Chem. Soc. 46 (2002) 52–56.
[14] M.J. McGlinchey, L. Girard, R. Ruffolo, Coord. Chem. Rev. 143 (1995) 331–381.
[15] K. Schlögl, H. Soukup, Monatsh. Chem. 99 (1968) 927–946.
[16] Y. Sasaki, C.U. Pittman Jr., J. Org. Chem. 38 (1973) 3723–3726.
[17] J.J.C. Erasmus, G.J. Lamprecht, J.C. Swarts, A. Roodt, A. Oskarsson, Acta Cryst. C 52 (1996) 3000–3002.
[18] H.K. Gupta, N. Reginato, F.O. Ogini, S. Brydges, M.J. McGlinchey, Can. J. Chem. 80 (2002) 1546–1554.
[19] (a) J. Kozikowski, R.E. Maginn, M.S. Klove, J. Am. Chem. Soc. 81 (1959) 2995–2997;
(b) E.O. Fischer, K. Pleszke, Chem. Ber. 91 (1958) 2719–2726.
[20] (a) L.P. Hammett, Chem. Rev. 16 (1935) 67–79;
(b) L.A. Flexser, L.P. Hammett, A. Dingwall, J. Am. Chem. Soc. 57 (1935) 2103–2115;
(c) L.P. Hammett, Chem. Rev. 13 (1933) 61–71;
(d) L.P. Hammett, M.A. Paul, J. Am. Chem. Soc. 56 (1934) 827–829;
(e) L.P. Hammett, A.J. Deyrup, J. Am. Chem. Soc. 55 (1933) 1900–1909;
(f) L.P. Hammett, A.J. Deyrup, J. Am. Chem. Soc. 54 (1932) 2721–2739.
[21] SMART and SAINT, Siemens AXS, Madison, WI, USA, 1995.
[22] G.M. Sheldrick, SADABS, University of Göttingen, Germany, 1996.
[23] SHEXTL 5, 10 ed. Bruker AXS Inc., Madison, WI, USA, 1997.
[24] L.J. Farrugia, J. Appl. Crystallogr. 30 (1997) 565.
[25] (a) G. Te Velde, F.M. Bickelhaupt, S.J.A. Van Gisbergen, C. Fonseca Guerra, J.G. Snijders, E.J. Baerends, T. Ziegler, J. Comput. Chem. 22 (2001) 931–967;
(b) C. Fonseca Guerra, J.G. Snijders, G. Te Velde, E.J. Baerends, Theor. Chem. Acc. 99 (1998) 391–403;
(c) ADF2006.01, SCM, Theoretical Chemistry, Vrije Universiteit, Amsterdam, The Netherlands. <http://www.scm.com>.
[26] (a) S.J.A. Van Gisbergen, J.G. Snijders, E.J. Baerends, Phys. Rev. Lett. 78 (1997) 3097–3100;
(b) S.J.A. Van Gisbergen, J.G. Snijders, E.J. Baerends, J. Chem. Phys. 109 (1998) 10644–10656.
[27] S.H. Vosko, L. Wilk, M. Nusair, Can. J. Phys. 58 (1980) 1200–1211.
[28] A.D. Becke, Phys. Rev. A 38 (1988) 3098–3100.
[29] J.P. Perdew, Phys. Rev. B 33 (1986) 8822–8824.
[30] (a) O.V. Gritsenko, P.R.T. Schipper, E.J. Baerends, Chem. Phys. Lett. 302 (1999) 199–207;
(b) P.R.T. Schipper, O.V. Gritsenko, S.J.A. van Gisbergen, E.J. Baerends, J. Chem. Phys. 112 (2000) 1344–1352.
[31] B.V. Rozynov, M.M. Teplyakov, V.P. Chebotarev, V.V. Korshak, Izv. Akad. Nauk SSSR Ser. Khim. (1974) 1602–1603.
[32] E.E. van Tamelen, I.L. Burkoth, J. Am. Chem. Soc. 89 (1967) 151–152.
[33] P. Štěpnička, I. Císařová, J. Sedláček, J. Vohlídal, M. Polášek, Collect. Czech. Chem. Commun. 62 (1997) 1577–1584.
[34] L.R. Snyder, J.J. Kirkland, J.L. Glajch, Practical HPLC Method Development, 2nd ed., Wiley, New York, 1997.
[35] (a) H.H. Tonnesen, J. Karlsen, A. Mostad, U. Penderson, P.B. Rasmussen, S.D. Lawesson, Acta Chem. Scand. Ser. B 37 (1983) 179–185;
(b) R.D.G. Jones, Acta Crystallogr., Sect. B 32 (1976) 1224–1227.
[36] (a) S.S. Elmorsy, A. Pelter, K. Smith, Tetrahedron Lett. 32 (1991) 4175–4176;
(b) S.S. Elmorsy, A. Pelter, K. Smith, M.B. Hursthoue, Tetrahedron Lett. 33 (1992) 821–824.
[37] G. Culbertson, R. Pettit, J. Am. Chem. Soc. 85 (1963) 741–743.